THE FRACTURE ENERGY OF COMPOSITE MATERIALS

Final Report

John O. Outwater
Michael C. Murphy

University of Vermont
Burlington, Vermont
September 1968

PICATINNY ARSENAL
DOVER, NEW JERSEY

The University of Vermont
Burlington, Vermont

THE FRACTURE ENERGY OF COMPOSITE MATERIALS

Contract No. DAAA 21-67-C-0041

FINAL REPORT

(September 1, 1967 to August 31, 1968)

By:

John O. Outwater and Michael C. Murphy

Submitted to:

U. S. Army Munitions Command
Picatinny Arsenal
Dover, New Jersey

September 30, 1968

Approved by: _____
J. O. Outwater
Principal Investigator

Table of Contents

LIST OF FIGURES

Fig. 13 A plot showing the effects of time in high temperature and humidity environment (165°F, 100% R.H.) on the debonding fracture energy between A-172* surface treated glass and resin.

Fig. 14 A plot showing the effects of time in a high temperature and humidity environment (165°F, 100% R.H.) on debonding fracture energy between Y-2525* surface treated glass and resin, and the rehealing effect of the glass-resin bond when re-exposed to an environment of laboratory air.

Fig. 15 A plot showing the effects of time in a high temperature and humidity environment (165°F, 100% R.H.) on debonding fracture energy between A-1100* surface treated glass and resin, and the rehealing effect of the glass-resin bond when re-exposed to an environment of laboratory air.

Fig. 16 A plot showing the effects of time in a high temperature and humidity environment (165°F, 100% R.H.) on debonding fracture energy between Y-2384* surface treated glass and resin, and the rehealing effect of the glass-resin bond when re-exposed to an environment of laboratory air.

*Union Carbide designation for surface treating agents.

FOREWORD

This report has been prepared by the University of Vermont under Contract No. DAAA 21-67-C-0041. Professor John O. Outwater was the Principal Investigator; he was assisted by Mr. Michael C. Murphy, Mr. John R. Chevalier and Mr. William O. Carnes.

The work is being administered under the direction of the Plastics and Packaging Laboratory, Feltman Research Laboratory, Picatinny Arsenal, Dover, New Jersey, with Dr. Elise McAbee as Contract Project Officer.

This final report covers the period September 1, 1967 to August 31, 1968, and summarizes various phases of the work on this contract mentioned in more detail in the earlier quarterly reports. It shows the theoretical foundations that the work will be guided along during the next 12 month period.

The results presented in this report represent work in progress and may be subject to revision as the program continues.

ABSTRACT

A study of the sources of the fracture energy and hence the brittleness of laminates shows that one of the parameters governing the usefulness of a filament as a reinforcement for a matrix is the debonding energy in shear, G_{II}, between the filament and the matrix. A novel method of measuring this value is described. Using this technique, values of G_{II} are determined for freshly drawn Pyrex rods with many different surface treatments embedded in anhydride cured epoxy resin. The effects of environment on G_{II} are shown and it is noted that all debonding energies tend to be substantially the same value after long exposure. The rate of decrease of G_{II} is essentially the same for all finishes and is linear down to a certain value when the rate of decrease is sharply reduced. The rate of decrease of G_{II} depends both on the humidity and the temperature.

INTRODUCTION

The fracture energy of a material is an important property. It indicates the energy required to extend a crack in that material and its numerical value is a measure of "the lack of brittleness" of the material. There are many techniques of measuring its value with homogeneous materials, but it is found that for many composites and particularly for glass reinforced plastics, the value of fracture energy is so high as to make its measurement impracticable by any of the present techniques.

The fracture energy of glass is about 0.04 lbs. per in., that of resin 1.26 lbs. per in., and that of reinforced plastics about 1,000 lbs. per in. The difference between the three is so great as to suggest a different mechanism from the usual direct methods of energy absorption.

Earlier work on this contract resulted in a theoretical prediction of the fracture energy of fiber reinforced composite materials which showed that a debonding of the fibers from the laminate was essential to this high fracture energy. The essence of the analysis rested in defining the depth of crack as the furthest distance to a load bearing filament regardless of the depth of crack through the resin alone. Such a definition is illustrated in Fig. 1. The fracture energy of the composite was computed on the basis of the total energy that could be absorbed by the debonded filaments as they were pulled to failure while the crack in the composite opened. This analysis gave the expression:

$$G_I = \frac{\sigma_f^2 A_f a}{4 E_f \tau} \left(\frac{\sigma_f}{A_f} - \sqrt{\frac{8 G_{II} E_f}{a}} \right)$$

where σ_f = stress in the filament,

A_f = area fraction of filament,

a = diameter of filament

E_f = modulus of filament

G_I = the opening mode fracture energy of the laminate

G_{II} = the shear mode fracture energy of debonding between the fiber and the resin.

τ = the frictional shear between the fiber and the resin matrix after debonding

This formula will apply whenever the fiber debonds within the resin matrix as the crack passes through the composite. There will be a slight additional energy involved if the crack does not follow a craze crack but, as the fracture energy of resin is so much less than that of the composite, the difference will be quite small.

This expression predicts the fracture energy of the laminate in terms of measurable quantities but it is dependent upon experimental values of G_{II} and τ which can be related to the surface properties of the fiber and the resin.

The measurement of G_{II} using different finishes and with different environments will be described below.

THE THEORETICAL DETERMINATION OF G_{II}

Fig. 2 sketches a single embedded fiber under a tensile load. As the fiber is loaded a debonded length x becomes apparent and this length will

gradually increase as the load on the fiber is increased. It can be related to various fiber parameters by:

$$(\sigma_f - 4\tau \frac{x}{a})^2 = \frac{8E_f}{a} G_{II}$$

It would be simple to measure G_{II} and τ were it possible to use a specimen of this sort. Unfortunately, it is not practicable to grip the end of the fiber without breaking it off. To circumvent the difficulties of gripping a fiber that might well be brittle, a compressive technique was devised using the specimen in Fig. 3.

This small compressive specimen upon analysis gives relationship of the debonding energy in the shear mode between the fiber and the resin as:

$$G_{II} = \left[(\sigma_r \frac{E_f}{E_r})^2 - (4\tau \frac{x}{a})^2 \right] \frac{a}{8E_f}$$

where E_r = Modulus of resin

Such specimens can readily be made by casting drawn and treated rods of glass in a plate of resin and subsequently milling this plate into small specimens approximately 1/2 in. by 1/2 in. by 1 in. These specimens are taken at random in groups of five and exposed to differing environments before being subjected to compression when the central fiber will debond from the matrix. The stress at which it debonds will give an indication of G_{II} and the increments of stress as the debonded line moves from the point of the fiber nearest the center of the specimen will give us a value of τ that is readily computable.

The unique advantages of this specimen is its simple construction, the simple evaluation of G_{II} and its small size enabling several specimens to be averaged.

When glass fiber was used in combination with the epoxy resin it was found that the fiber would debond explosively when a certain critical stress in the resin was reached. This indicates that τ was small and we would be well justified in ignoring it on glass resin systems thereby simplifying the expression to:

$$G_{II} = \frac{\sigma_r^2 E_f a}{8 E_r^2}$$

The influence of the environment on the value of G_{II} is a measure of the usefulness of a finish for glass. Using this technique we have explored the effects of different environments on a variety of commonly used finishes.

EXPERIMENTAL RESULTS

The test specimens were made by embedding freshly drawn Pyrex rods that had been treated with various finishing agents in resin. Six rods were embedded at a time and the resulting casting could be cut up to make 36 specimens after they had been drilled through the center to cut the rod. The specimens were then selected at random in groups of five using a random number table so that each published value of fracture energy in shear would be an average of five readings.

The resins used were expoxy and polyester. It was found, however, that polyester resin shrank so severely on curing that cracks were evident criss-crossing the casting and cracks also appeared along the whole length of the various rods. This cracking could not be prevented so any readings obtained with polyester resin would be futile. It has

been shown earlier that this behavior is usual with polyester resins as their shrinkage is always much greater than that with epoxy resins and may be as much as 20%. The resin used in all the tests then was 100 parts Epon 826, 90 parts Nadic methyl anhydride and 1 part DMBA. It was cured at 250°F for 24 hrs. before cooling to room temperature and cutting into smaller specimens.

The results are shown in Table 1 and are illuminating in that different finishes result with substantially different values of G_{II}. Particularly the A-150 and A-172, Y-2384 and Y-4148 finishes give distinctly lower values of G_{II} than rods with other treatments or with no treatment. The most common treatment A-1100 gives a value of G_{II} substantially the same as that of untreated glass.

The next problem was to measure the effects of various environments. The specimens were exposed to different atmospheres for increasing periods of time and the effects of time on different surface treatments could be plotted in Figs. 4, 5, 6, 7, 8, 9, 10, 11, 12, 13, 14, 15, and 16. The results are interesting in that the decline of the fracture energy in shear was linear with time until a certain low level had been reached and then it remained substantially constant though decreasing slowly. The rate of decrease was substantially the same for all finishes and also for no finish at all unless the fracture energy was quite low to start with--as with the finishes mentioned above. The effects of lower humidity are shown in Figs. 5 and 6. The rate of decline is strongly dependent on the humidity as might be suspected but, more particularly, it seems vitally dependent on the temperature as the effects of sea water at room temperature were small. It was suspected that the values might improve if the specimens were removed from the hot humid

atmosphere and exposed to laboratory air. There was limited improvement as the value of G_{II} stayed at the low level with small increase. This is shown in Figs. 14, 15 and 16.

DISCUSSION

The values of G_{II} measured above and the changes that they reveal in the presence of moisture may be of profound importance in the understanding of reinforced plastics. Particularly we can see that, regardless of the finish, we obtain the same low value of G_{II} after long exposure. The fact that the fracture energy decreases linearly with time suggests a diffusion mechanism and it may well be that G_{II} is controlled by the diffusion of moisture to the interface. This will be checked later. The low value of G_{II} implies that there is little bonding indeed between the filament and the matrix after exposure and, as we have discussed in earlier reports, the controlling parameters in regard to the fracture energy or brittlemess of a laminate are those that decide whether the filament will debond before its own fracture or whether the crack in the resin will cause the filament to break without debonding along its length. The fact that we will obtain a low value of fracture energy in shear between the matrix and the fiber with the materials chosen implies that we have more latitude than we had expected in the choice of resins and finishes to give non-brittle laminates. In fact, unless we use fibers of small diameter, we cannot expect glass fibers to give other than a tough laminate.

We tested this hypothesis further by embedding boron filaments in epoxy resin. There was no debonding before fracture of the fiber and,

indeed, the debonding energy in shear could not be measured. We would expect a brittle laminate and this was just what we found: a crack in the resin went straight across the filament so that the filament had no apparent crack stopping ability.

Efforts were also made to measure the debonding energy in shear of stainless steel wires in epoxy resin. It was not possible to measure G_{II} for these filaments using our present technique. It appeared that the wires bonded so securely that they were always deformed plastically when a laminate was broken. In this case we would again obtain a tough laminate but the mechanism, instead of being due to debonding, would be due to the energy absorption in the plastic deformation of the reinforcing wires.

CONCLUSIONS

The measurement of the debonding energy in shear between a filament and resin for various surface finishes on glass rods shows the values of G_{II} are different for different finishes and that all finishes lead to about the same value of G_{II} after a long exposure. The rate of change depends on temperature as well as on humidity so, if we are to test reinforced plastics for mechanical properties, we must either expect the properties to change with exposure or we must thoroughly expose them to a hot humid environment before testing.

TABLE I

A table of fracture energies, G_{II}, for selected surface treatments applied to finely drawn Pyrex glass fibers embedded in resin of composition--100 pts. EPON 826, 90 pts. NADIC Methyl Anhydride, 1 pt. DMBA--cured at 250 F°for 24 hours.

SURFACE TREATMENT	G_{II} in-lb/in^2
A-150 vinyltrichlorosilane	3.6
A-151 vinyltriethoxysilane	13.3
A-172 vinyltris (beta methoxyethoxy) silane	4.9
Y-2525 vinyltrimethoxysilane	22.3
Y-2384 vinyltriacetoxysilane	9.1
A-1100 gamma aminopropyltriethoxysilane	23.3
Y-2967 N,N bis (beta hydroxy ethyl) gamma aminopropyltriethoxysilane	24.6
Y-4086 beta (3,4 epoxy cyclohexyl) ethyltrimethoxysilane	22.6
Y-4087 gamma glycidoxypropyltrimethoxysilane	25.9
A-174 gamma methacryloxypropyltrimethoxysilane	17.6
Y-4148 gamma methacryloxypropyltrichlorosilane	9.1
NONE	22.5

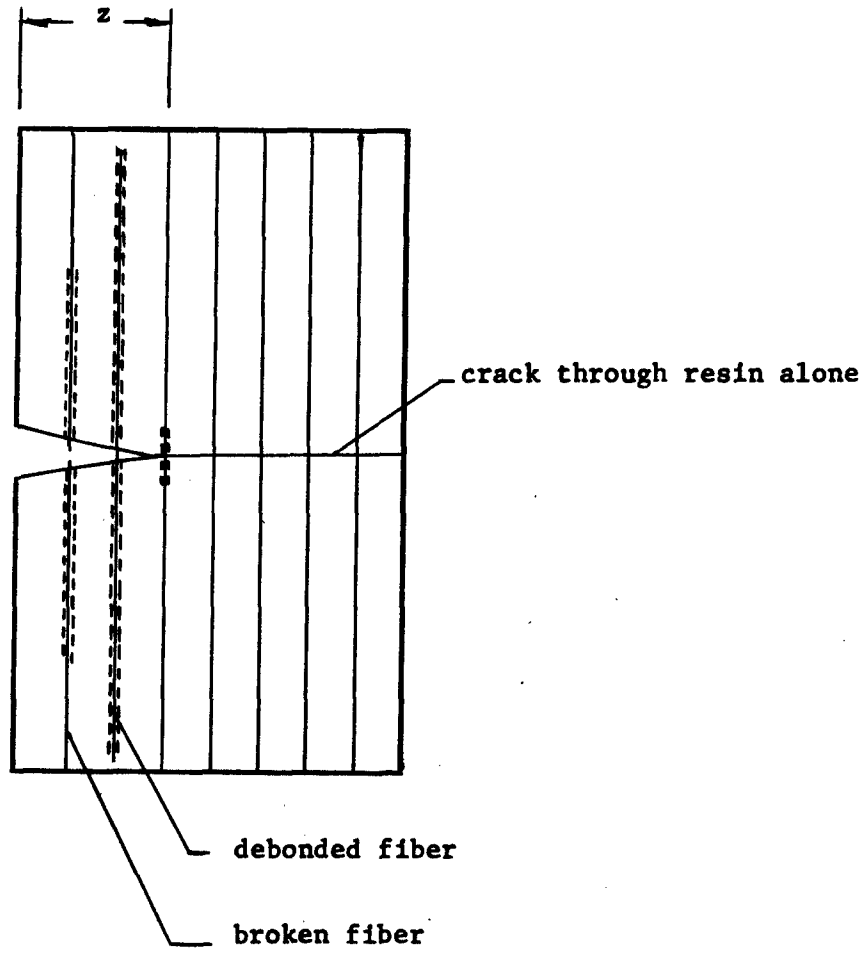

Fig. 1 A sketch illustrating the definition of crack depth, z, in a laminate.

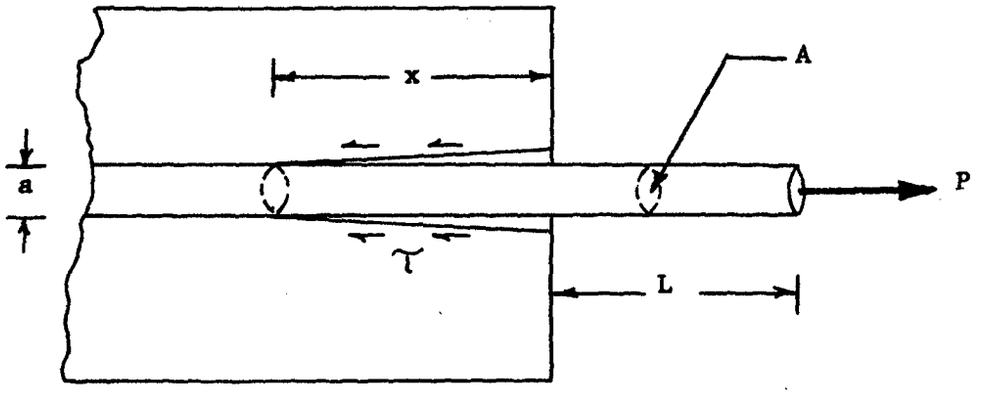

Fig. 2. Sketch of a single embedded fiber under tensile load.

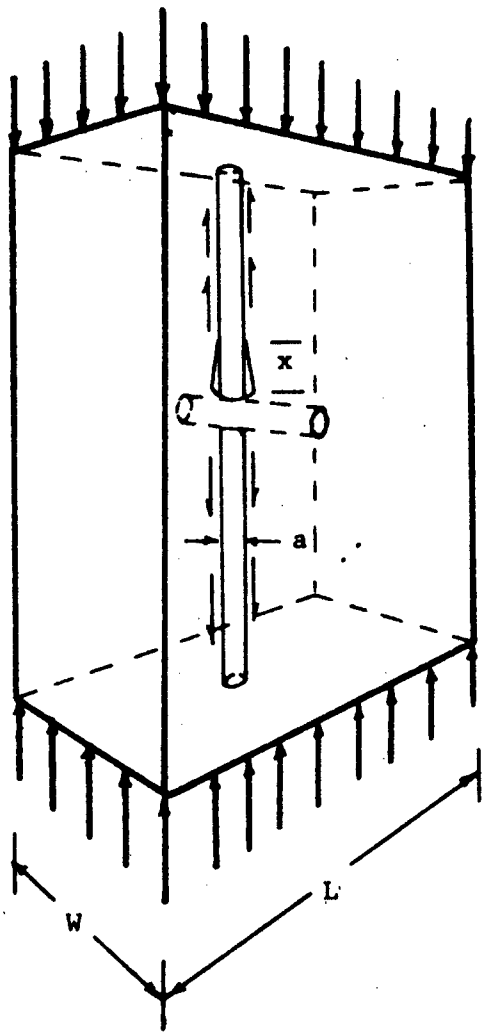

Fig. 3 Sketch of technique used to determine the debonding fracture energy between the resin and the fiber.

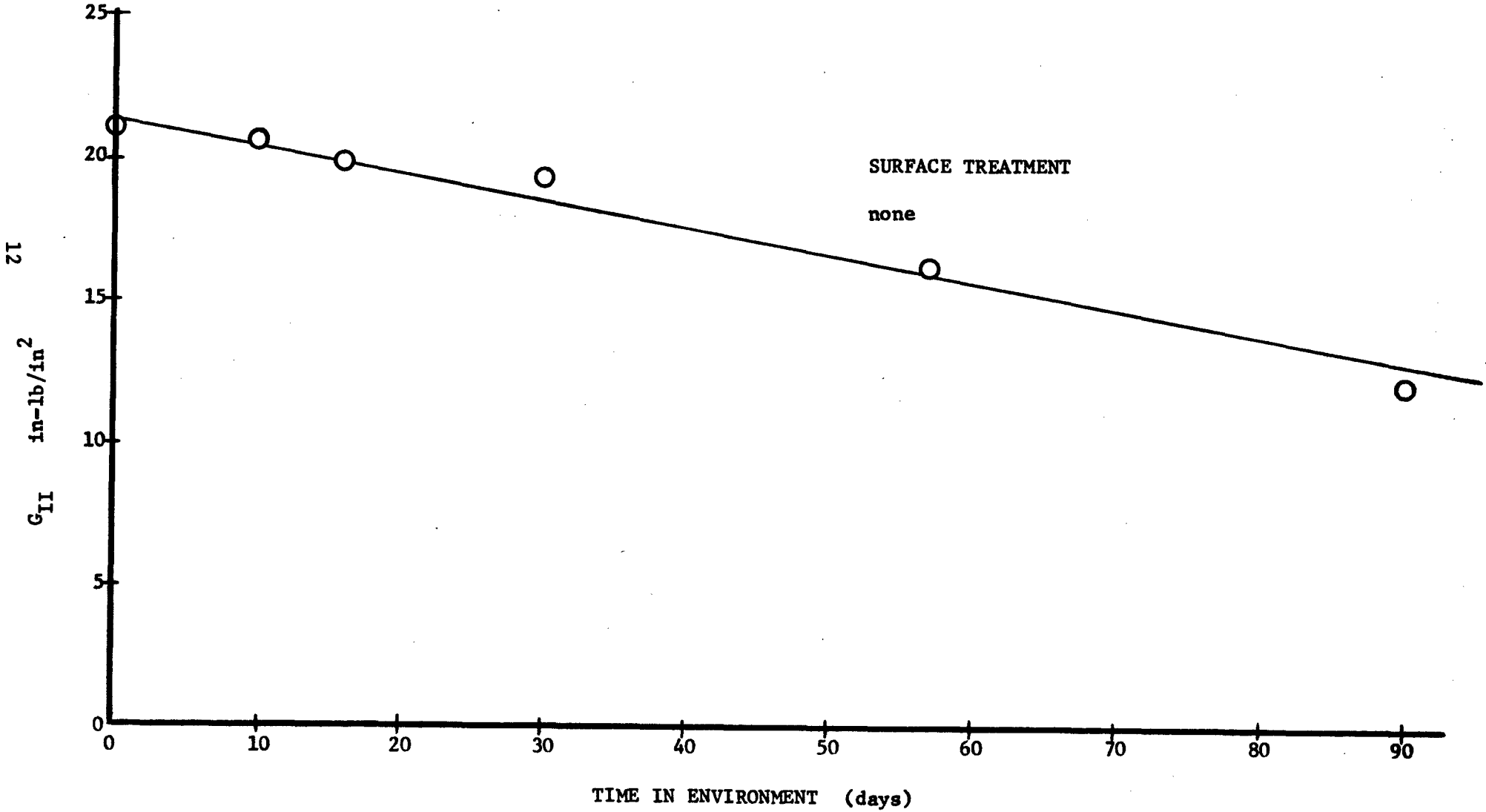

Fig. 4 A plot showing the effect of time in a rust contaminated salt water environment on the debonding fracture energy between glass and resin.

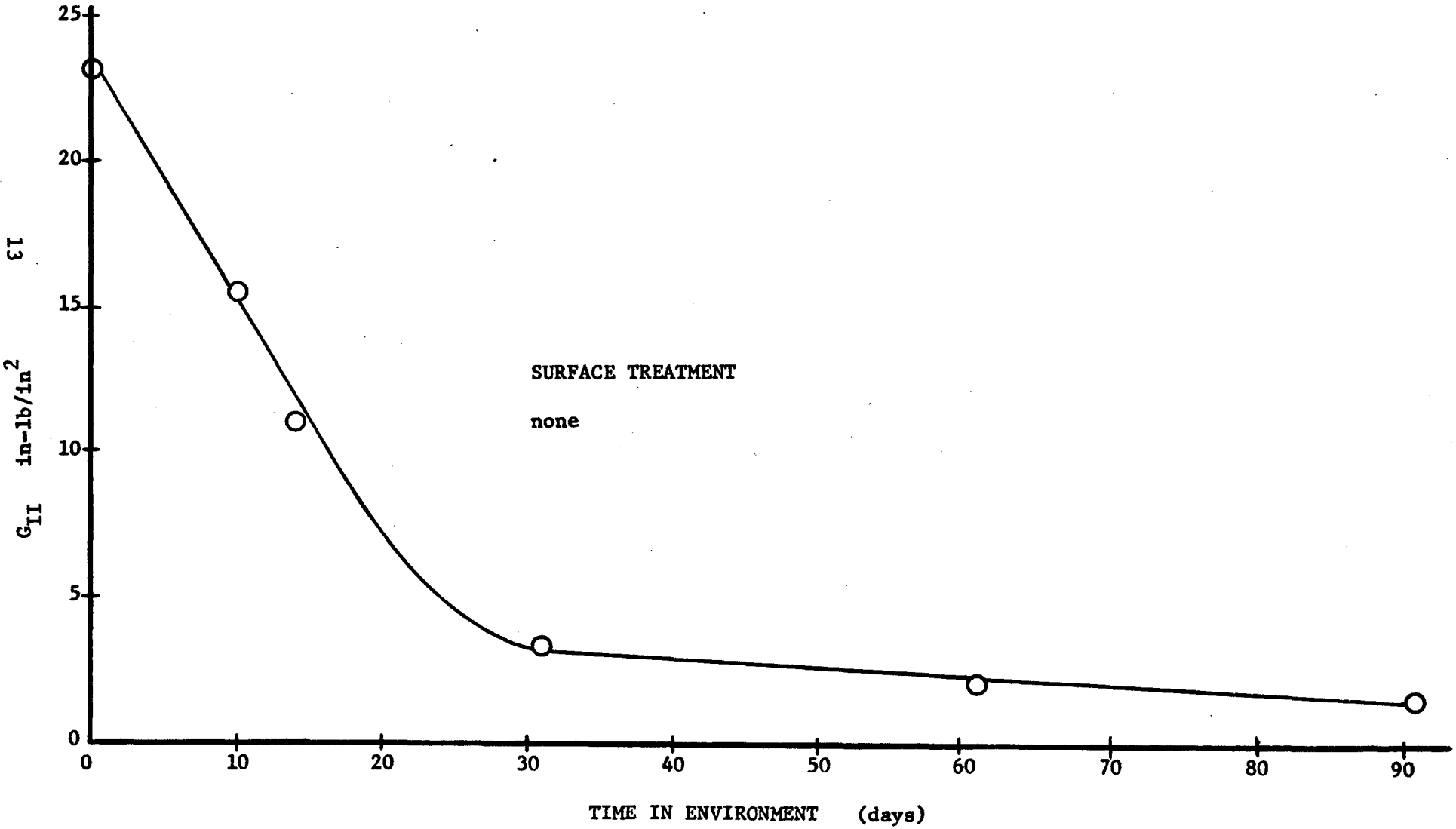

Fig. 5 A plot showing the effect of time in a high temperature and humidity environment (165°F, 25% R.H.) on the debonding fracture energy between glass and resin.

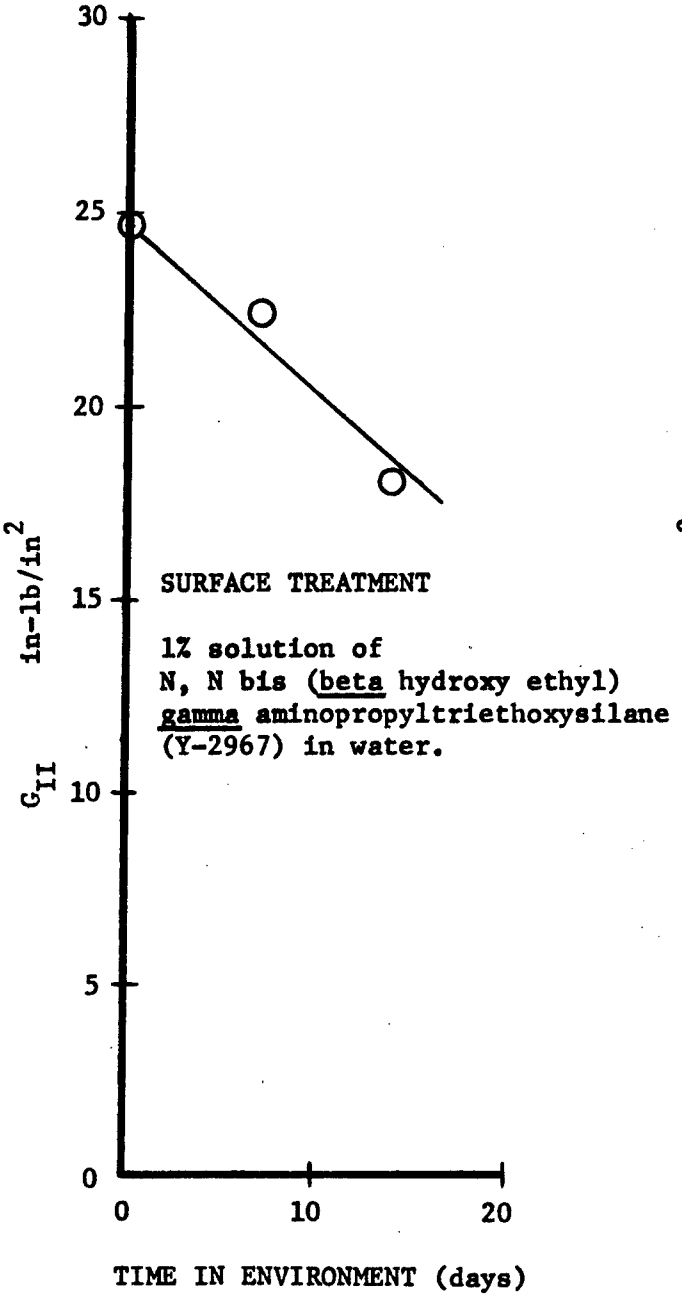

Fig. 6 A plot showing the effects of time in high temperature and humidity environment (165°F, 25% R.H.) on the debonding fracture energy between glass and resin.

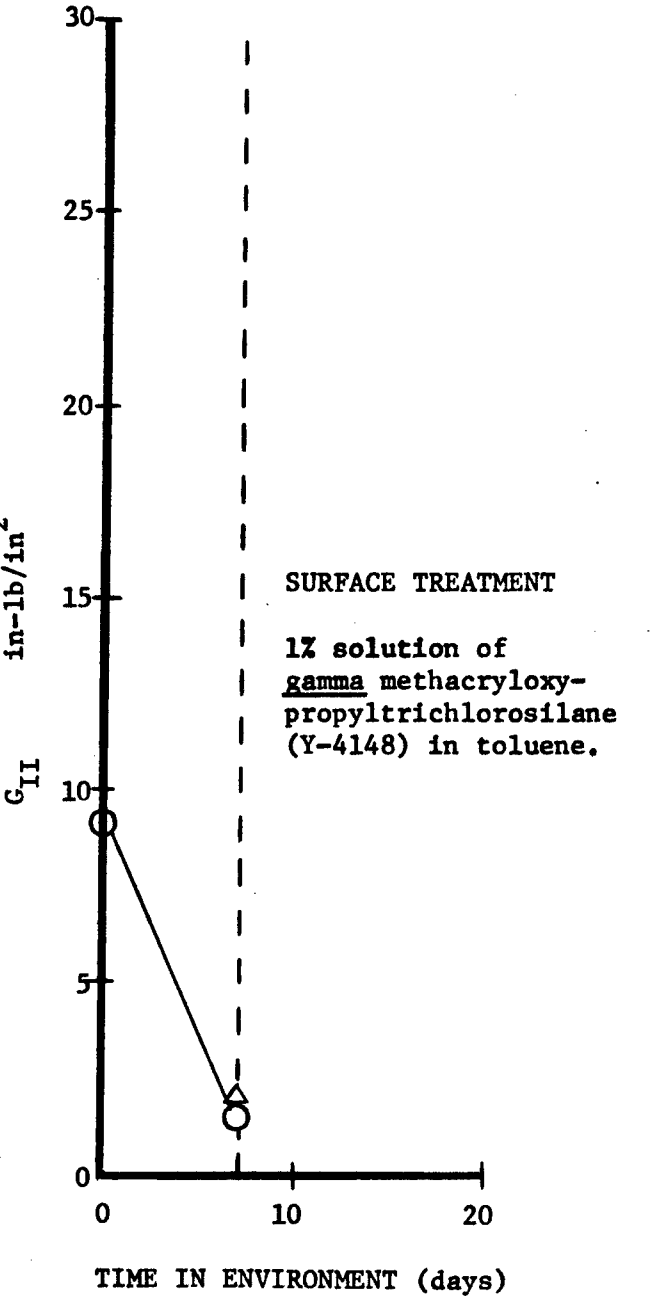

Fig. 7 A plot showing the effects of time in high temperature and humidity environment (165°F, 100% R.H.) on the debonding fracture energy between glass and resin. △ indicates rehealing effect of 4 hr. post-cure at 250°F.

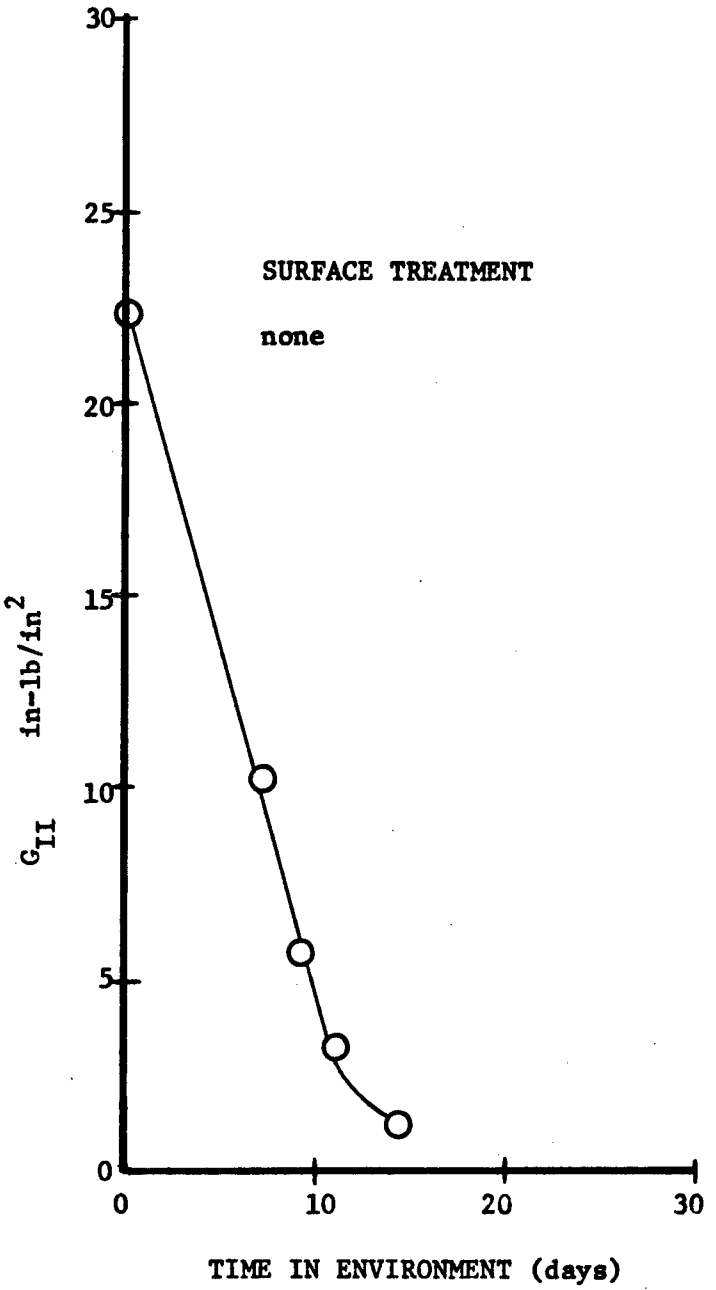

Fig. 8 A plot showing the effects of time in high temperature and humidity environment (165°F, 100% R.H.) on the debonding fracture energy between glass and resin.

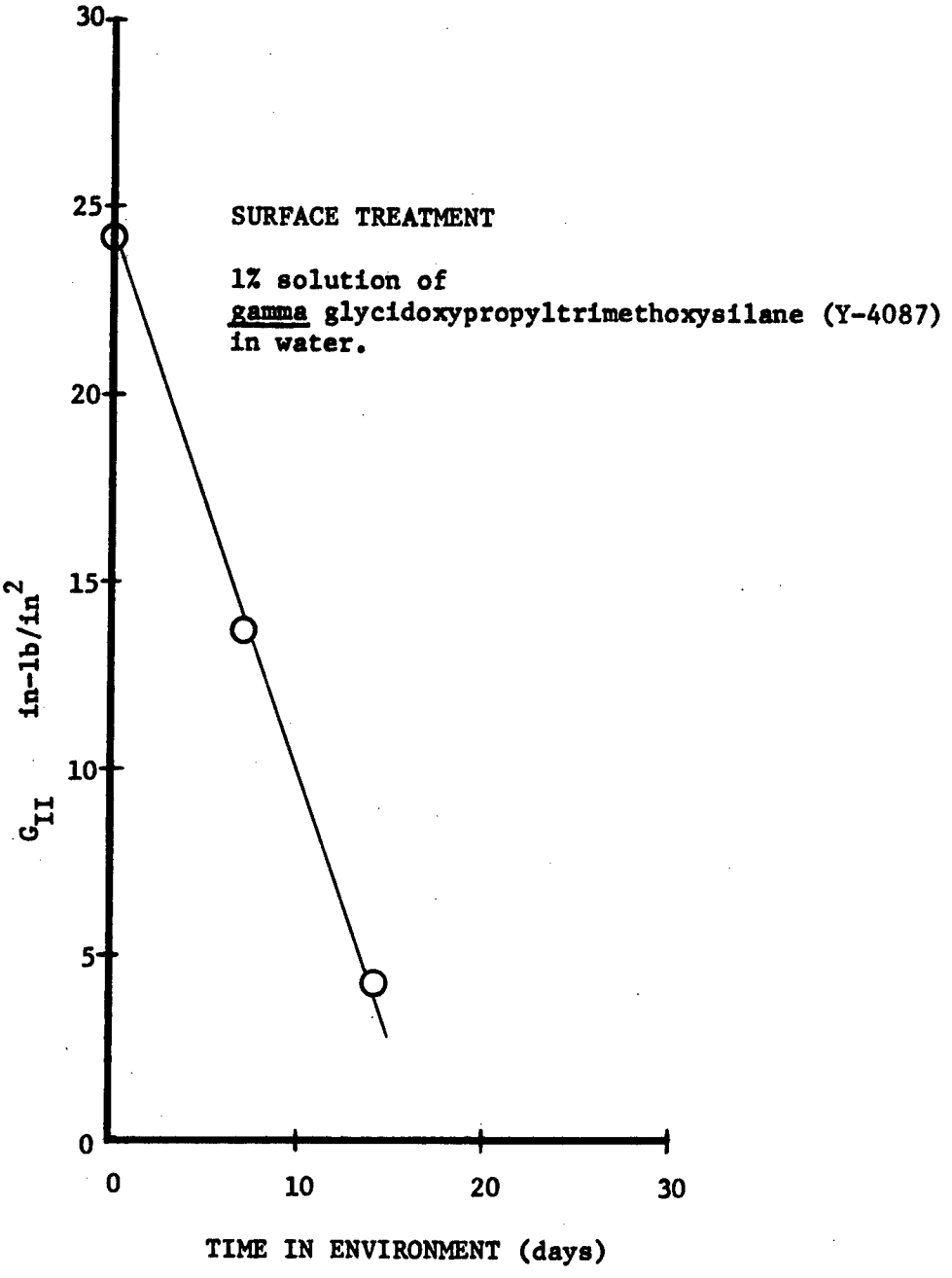

Fig. 9 A plot showing the effects of time in high temperature and humidity environment (165°F, 100% R.H.) on the debonding fracture energy between glass and resin.

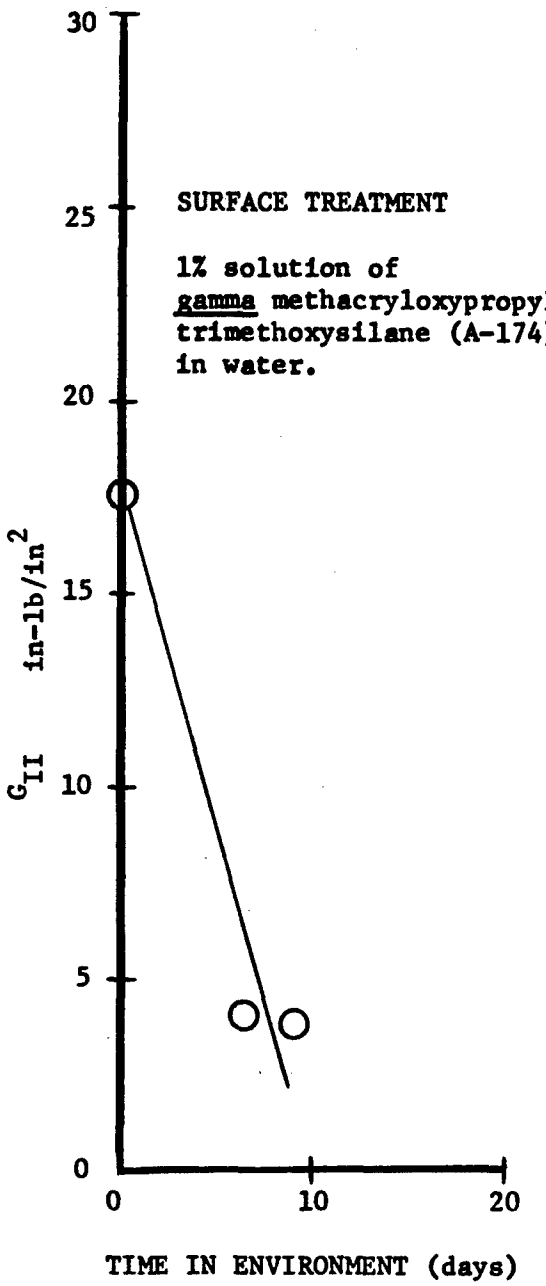

Fig. 10

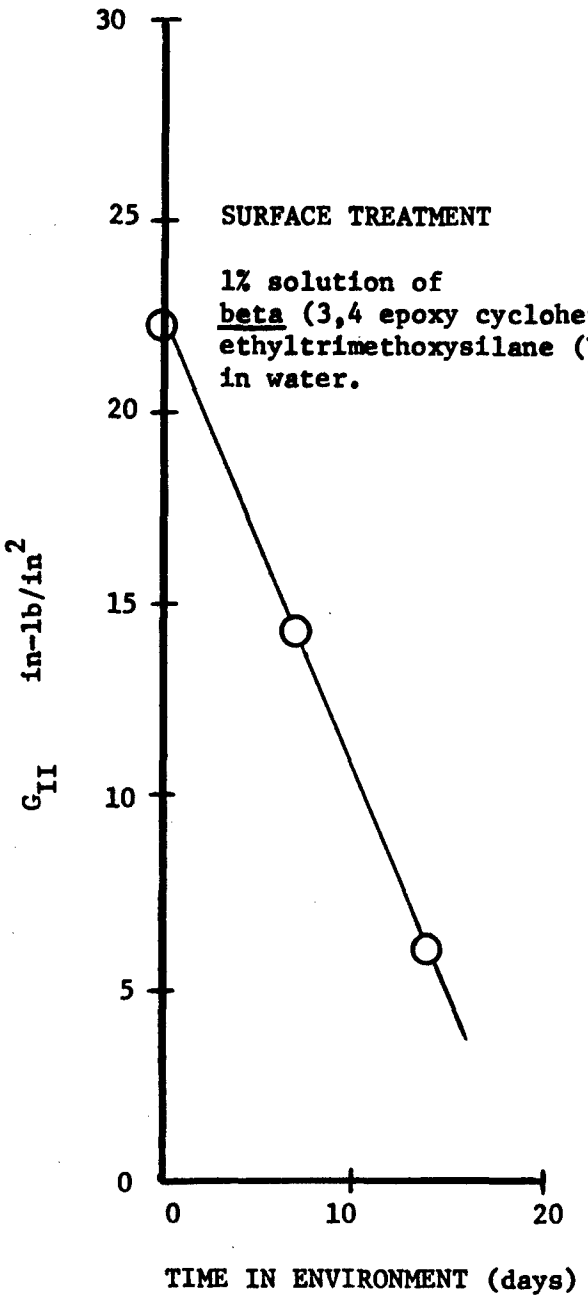

Fig. 11

Plots showing the effects of time in high temperature and humidity environment (165°F, 100% R.H.) on the debonding fracture energy between glass and resin.

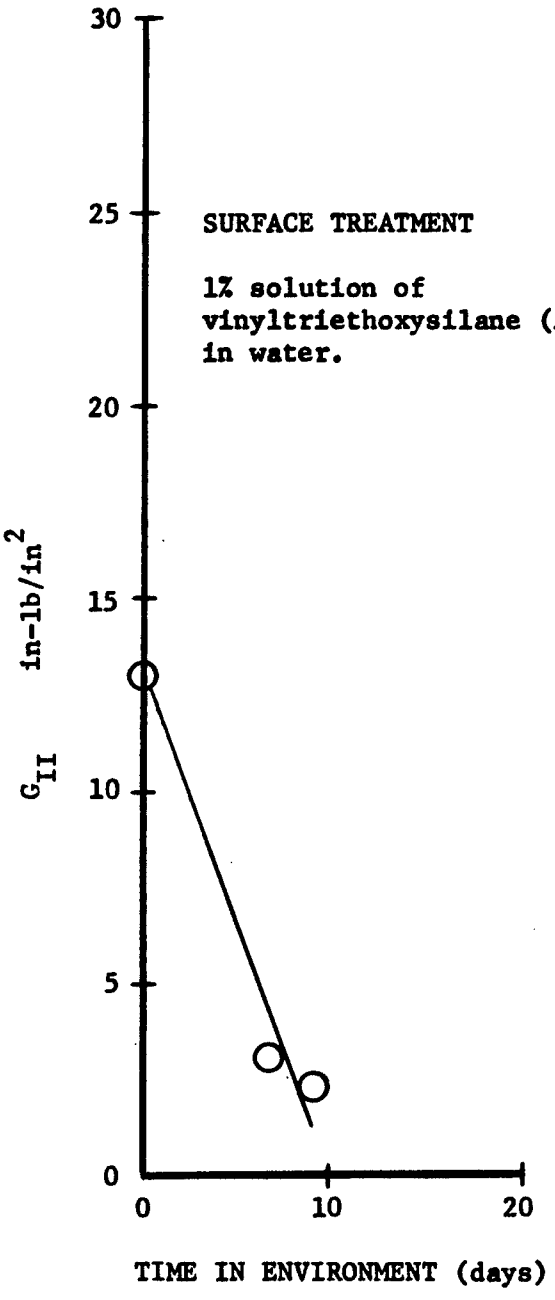

Fig. 12

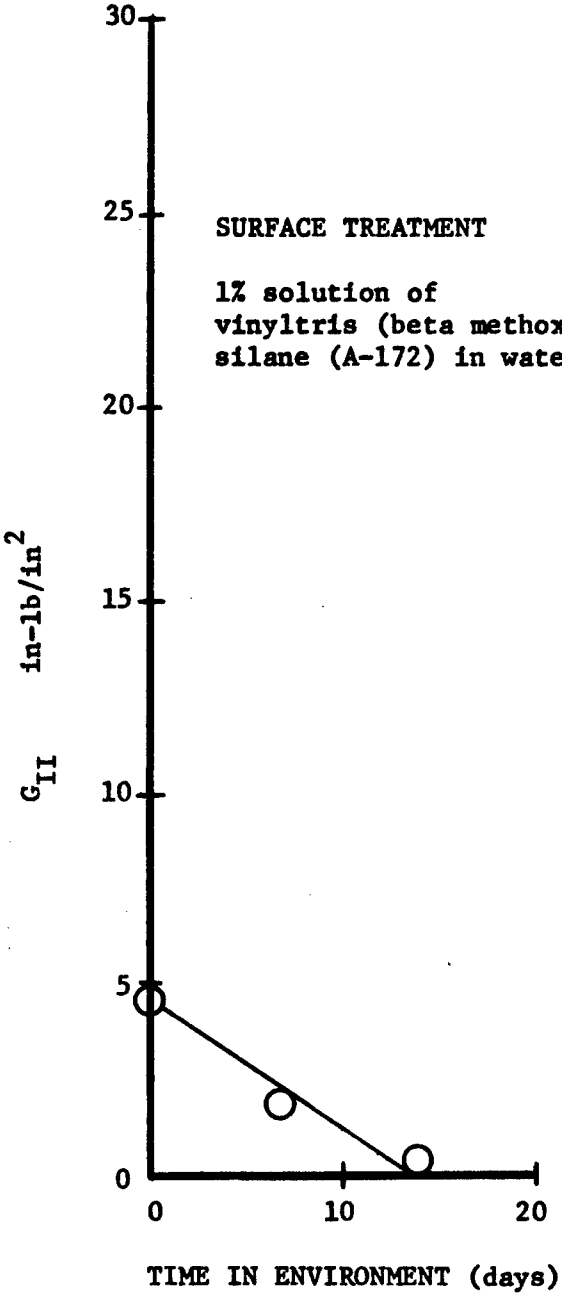

Fig. 13

Plots showing the effects of time in high temperature and humidity environment (165°F, 100% R.H.) on the debonding fracture energy between glass and resin.

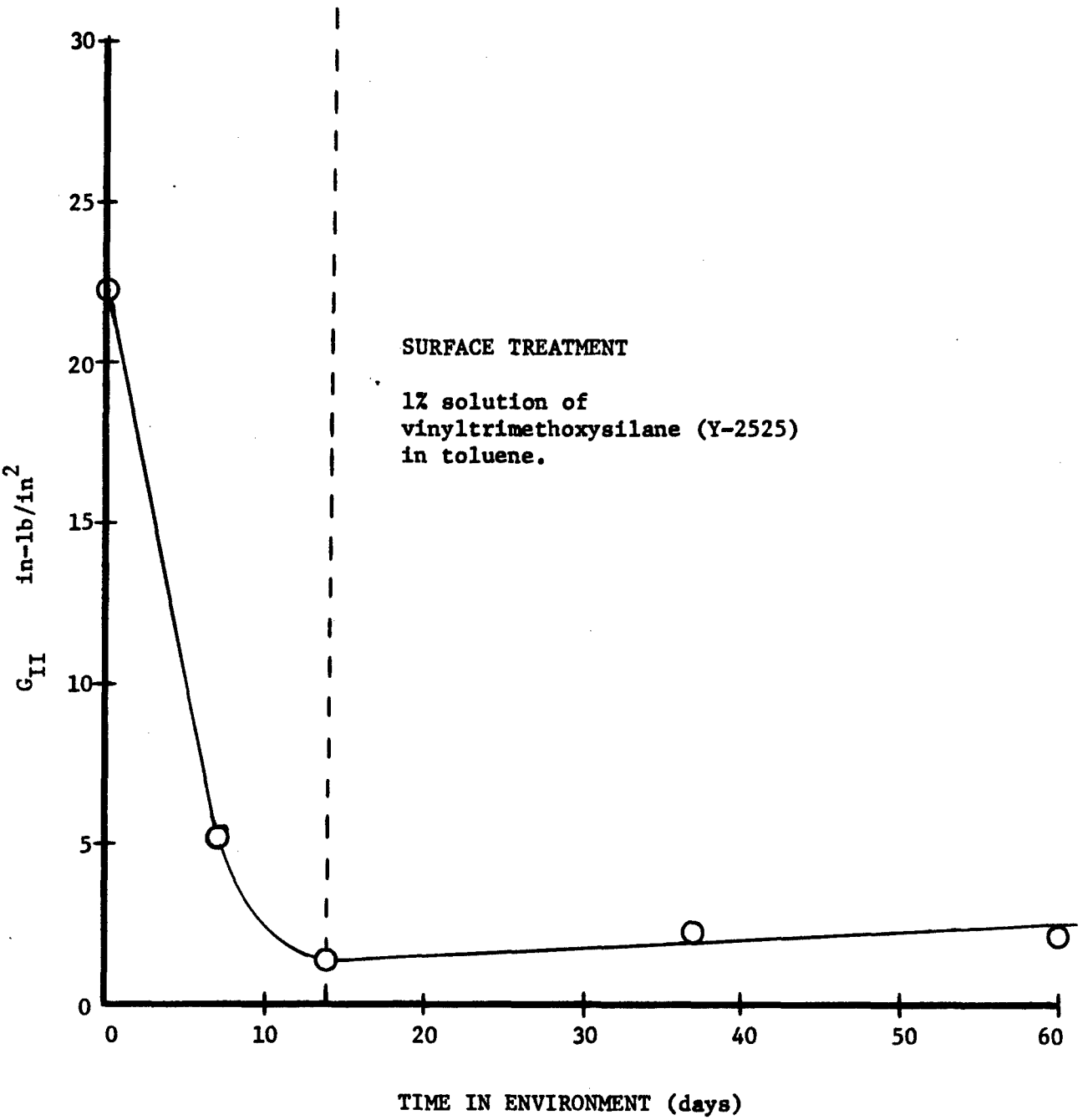

Fig. 14 A plot showing the effects of time in high temperature and humidity environment (165°F, 100% R.H.) on the debonding fracture energy between glass and resin (left of dashed line), and the rehealing effect of the glass-resin bond when reexposed to an environment of laboratory air (right of dashed line).

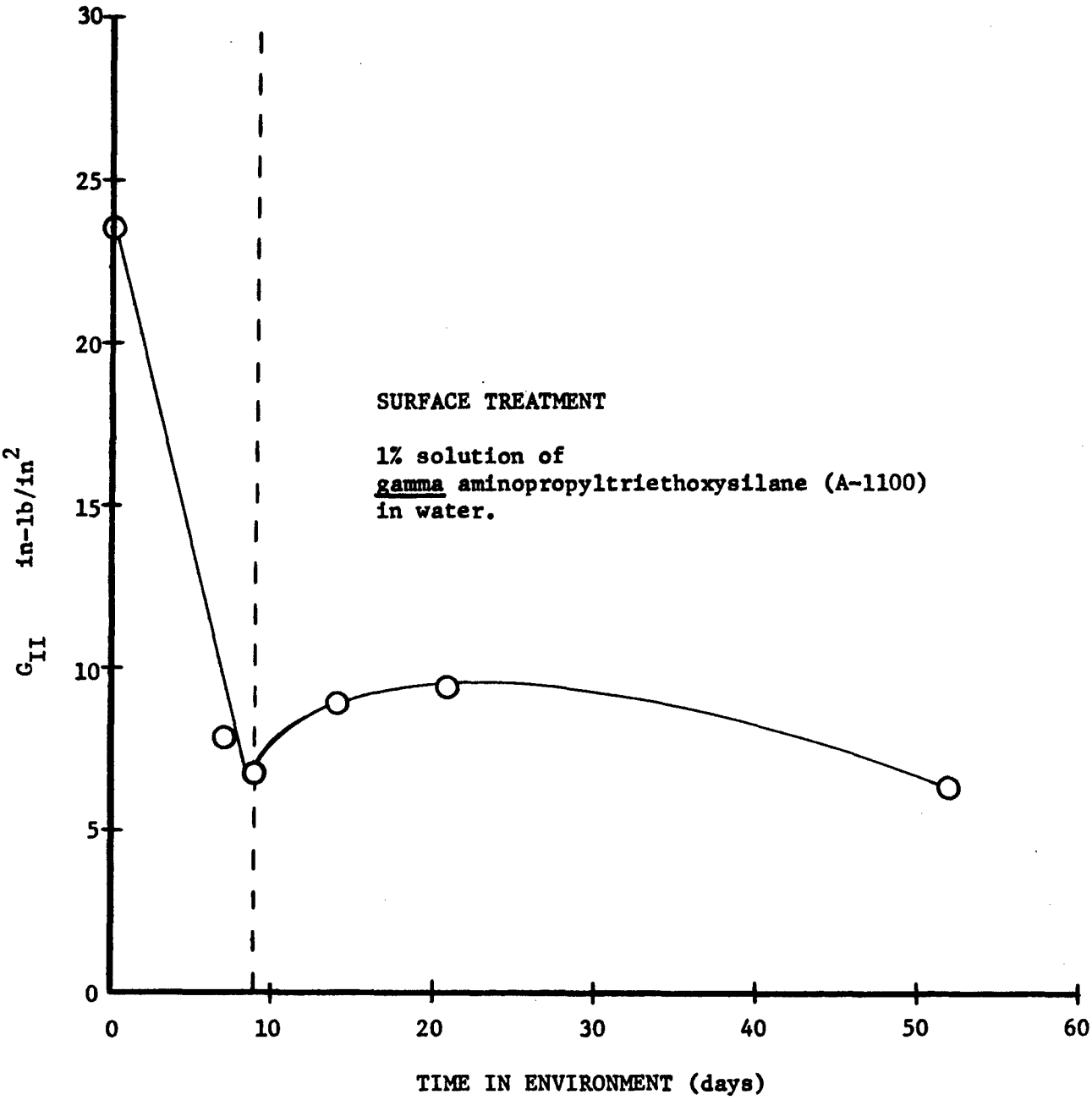

Fig. 15 A plot showing the effects of time in high temperature and humidity environment (165°F, 100% R.H.) on the debonding fracture energy between glass and resin (left of dashed line), and the rehealing effect of the glass-resin bond when reexposed to an environment of laboratory air (right of dashed line).

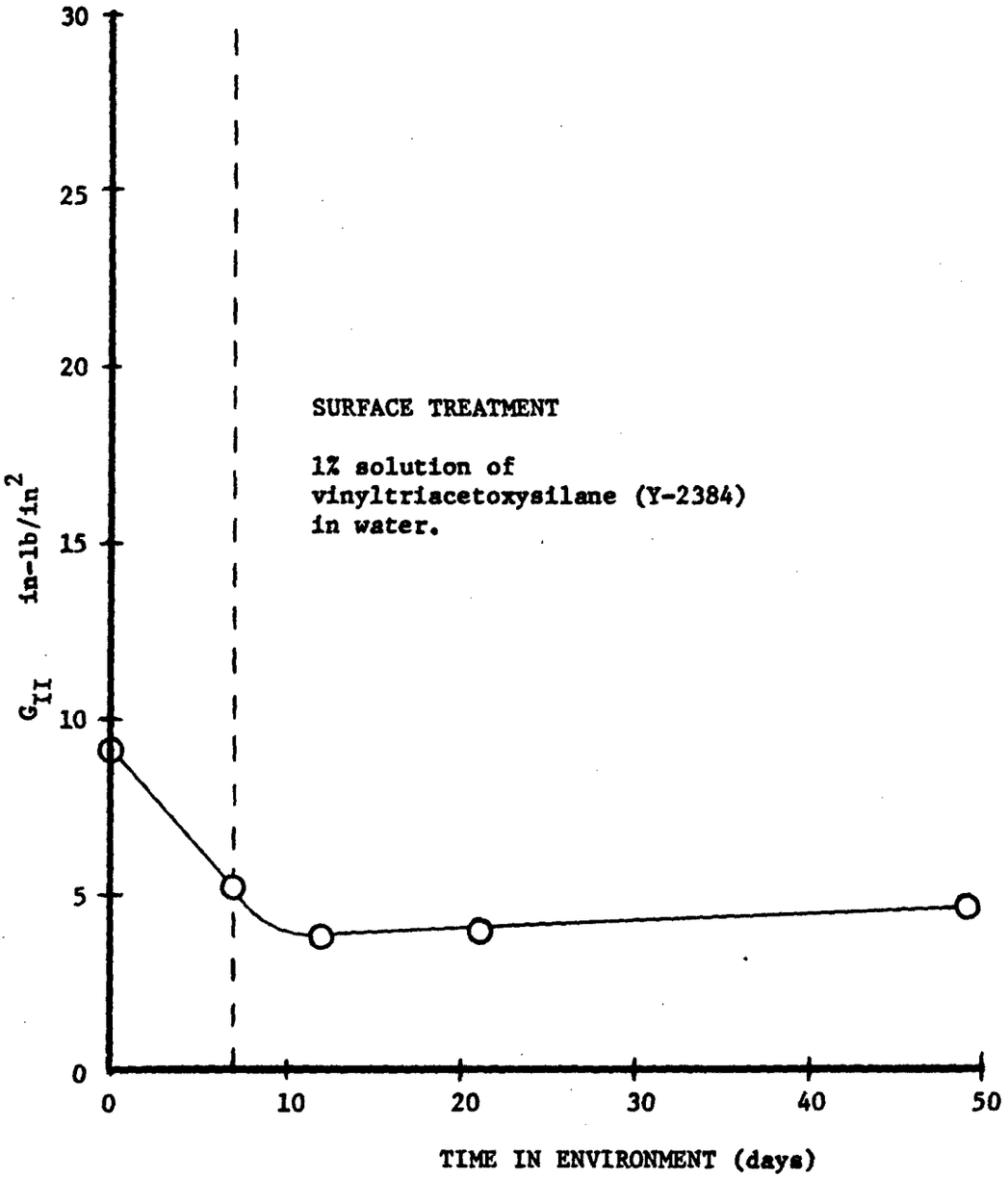

Fig. 16 A plot showing the effects of time in high temperature and humidity environment (165°F, 100% R.H.) on the debonding fracture energy between glass and resin (left of dashed line), and the rehealing effect of the glass-resin bond when reexposed to an environment of laboratory air (right of dashed line).

BIBLIOGRAPHY

1. Outwater, J. O. and Carnes, W. O. Fracture Energy of Composite Materials. Final Report on Contract No. DAAA-21-67-C-0041, U.S. Army Munitions Command, Picatinny Arsenal, 1967.

2. Outwater, J. O., Carnes, W. O. and Murphy, M. C. Fracture Energy of Composite Materials. Quarterly Report (December) on Contract No. DAAA-21-67-C-0041, U.S. Army Munitions Command, Picatinny Arsenal, 1967.

3. Outwater, J. O., Carnes, W. O. and Murphy, M. C. Fracture Energy of Composite Materials. Quarterly Report (March) on Contract No. DAAA-21-67-0041, U. S. Army Munitions Command, Picatinny Arsenal, 1968.

4. Outwater, J. O., Carnes, W. O. and Murphy, Fracture Energy of Composite Materials, Quarterly Report (June) on Contract No. DAAA-21-67-0041, U.S. Army Munitions Command, Picatinny Arsenal 1968.

5. Outwater, J. O. and Carnes, W. O. The Fracture Mechanics of Composite Materials, Proceedings of the Army Symposium on Solid Mechanics, 1968.

DISTRIBUTION LIST

	Copy No.
Commanding Officer Picatinny Arsenal ATTN: Procurement Division P & P Directorate - SMUPA - PA13 Dover, New Jersey 07801	1-6
Commanding General Army Material Command ATTN: AMCRD-RD, Dr. Peter Kosting Mr. J. Beebe Washington, D.C. 20315	7 8
Commanding General U. S. Army Munitions Command ATTN: AMSMU-RE Dover, New Jersey 07801	9
Plastics Technical Evaluation Center ATTN: Chief, Mr. H. Pebly Picatinny Arsenal Dover, New Jersey 07801	10-11
Commanding General U. S. Army Weapons Command ATTN: AMSWE-RDR Rock Island, Illinois	12-13
Redstone Scientific Information Center U. S. Army Missile Command ATTN: Chief, Document Section Redstone Arsenal, Alabama 35808	14-15
Sandia Corporation Sandia Base ATTN: Bertha R. Allen Albuquerque, New Mexico	16
Sandia Corporation Livermore Laboratory ATTN: Librarian P. O. Box 969 Livermore, California	17
U. S. Army Transportation Research Command ATTN: Mr. N. C. Thomas Mr. F. P. McCourt Dr. Echols Fort Eustis, Virginia	18 19 20

	Copy No.
Interservice Data Exchange Program **AOMC IDEP Office** **ATTN: Mr. Schenk** **Redstone Arsenal, Alabama**	21-31
Commandant U. S. Army Ordnance Center and School ATTN: AISO-SL Aberdeen Proving Ground, Maryland 21005	32
U. S. Naval Avionics Facility Materials Laboratory and Consultants Division ATTN: Paul H. Guhl, Organic Materials Br., RDM-3 Indianapolis, Indiana 46218	33
Commanding Officer U. S. Army Edgewood Arsenal ATTN: Mr. Milton A. Raun, Chief, Development Engineering Branch Edgewood Arsenal, Maryland 21010	34
Commanding General Natick Laboratories ATTN: Clothing and Organic Materials Division Natick, Massachusetts	35-37
Commanding Officer U. S. Army Transportation Research Command ATTN: ASE (Mr. J. E. Forehand) Fort Eustis, Virginia	38
Department of the Navy Office of Naval Research ATTN: Code 423 Washington 25, D. C.	39
Commanding Officer Watervliet Arsenal ATTN: T. E. Davidson, Chief, Phys. & Mech. Metallurgy Lab Watervliet, New York	40
Commanding General U. S. Army Missile Command ATTN: Mr. Julian Kobler, AMSMI-RSX Redstone Arsenal, Alabama	41
Department of the Navy Bureau of Ships Hull Division Materials Development and Applications Branch ATTN: Mr. J. B. Alfers, Code 634C Washington 25, D. C.	42

	Copy No.
U. S. Naval Ordnance Laboratory ATTN: Mr. H. A. Perry Mr. F. R. Barnet, Chief, Nonmetallic Materials Division Silver Spring, Maryland 20910	43 44
Director U. S. Naval Research Laboratory ATTN: Code 1017 Washington, D. C. 20390	45
Department of the Navy Bureau of Naval Weapons ATTN: RRMA Airborne Equipment Division Washington 25, D. C.	46 47
Director U. S. Navy Applied Science Laboratory Navy Base Brooklyn, New York	48
Department of the Navy Bureau of Supplies and Accounts ATTN: Code H32 Washington, D. C. 20360	49
Commanding Officer U. S. Naval Weapons Station ATTN: Mr. U. Cormier, Director, Research and Development Division Yorktown, Virginia	50
Mr. E. K. Rishel, Head, Plastics Branch Aeronautical Materials Laboratory Naval Air Engineering Center Building 76-5 Philadelphia 12, Pennsylvania	51
Naval Weapons Laboratory ATTN: Mr. R. Tom (Code WCD) Dahlgren, Virginia 22448	52
Department of the Navy Bureau of Naval Weapons ATTN: Mr. P. M. Goodwin, RRMA-10 Washington 25, D. C.	53
Naval Air Development Center Aeronautical, Electronic, and Electrical Laboratory ATTN: Dr. H. R. Moore, Head, Materials & Process Branch Johnsville, Pennsylvania	54

	Copy No.
Commander (Code 5557) U. S. Naval Ordnance Test Station China Lake, California 93557	55
David Taylor Model Basin ATTN: Mr. A. R. Willner, Materials Research Branch Washington 7, D. C.	56
Commander Aeronautical Systems Division Wright-Patterson Air Force Base ATTN: Mr. R. T. Schwartz, MANC Dayton, Ohio 45433	57
Defense Documentation Center Cameron Station Alexandria, Virginia 22314	58-77
Dr. W. R. Lucas (M-P and VE-M) George C. Marshall Space Flight Center Huntsville, Alabama 35800	78
Department of Commerce National Bureau of Standards Room 4022, Industrial Building Washington, D. C. 20324	79
Commandant U. S. Army Ordnance Guided Missile School ATTN: AJQ-OT, Feedback Section Redstone Arsenal, Alabama	80
Commanding Officer Ammunition Procurement and Supply Agency ATTN: SMUAP-QFO Joliet, Illinois 60400	81
Commanding Officer Army Materials and Mechanics Research Center Watertown Arsenal ATTN: Technical Information Center Watertown, Mass. 02172	82
Commanding Officer Harry Diamond Laboratories ATTN: Library, Room 211, Building 92 Connecticut Avenue and Van Ness Street, NW Washington, D. C. 20438	83
Commanding General U. S. Army Electronics Command ATTN: SIG-FM/EL-PEM-1-d Mr. Gerald Platon Fort Monmouth, New Jersey 07703	84 85

	Copy No.
Commanding Officer ATTN: SMUEA-TO-DA (Mr. Cooke) Edgewood Arsenal, Maryland	86
Commanding Officer Engineer Research and Development Laboratories Materials Branch ATTN: Mr. Philip Mitton Mr. S. Goldfein Information Resources Branch Fort Belvoir, Virginia	87 88 89
Commanding Officer U. S. Army Tank-Automotive Center ATTN: SMOTA-RCM. 3, Mr. David R. Lem SMOTA-RTS, Technical Data Coordination Warren, Michigan 48090	90 91
Commanding Officer Aberdeen Proving Ground ATTN: Technical Library, Building 303 Maryland 21005	92-93
Director U. S. Army Coating and Chemical Laboratory Aberdeen Proving Ground, Maryland 21005	94
Commanding General White Sands Missile Range ATTN: Technical Librarian New Mexico 88002	95
Commanding Officer Frankford Arsenal ATTN: Pitman-Dunn Labs, Dr. H. Gisser Library Branch, 0270 Philadelphia, Pennsylvania	96 97
Commanding Officer Rock Island Arsenal ATTN: Laboratory, Mr. R. F. Shaw Rock Island, Illinois	98
Commanding Officer Springfield Armory ATTN: Res Chem Lab, Mr. Zavarella Springfield 1, Massachusetts	99

	Copy No.
Commanding Officer Watervliet Arsenal ATTN: Mr. Fred Schmiedeshoff Watervliet, New York 13601	100
Commanding Officer Harry Diamond Laboratories ATTN: Mr. Asaf Benderly Connecticut Avenue and Van Ness Street, N.W. Washington, D. C. 20438	101
Commanding Officer U. S. Army Tank and Automative Center ATTN: Mr. Charles Green Warren, Michigan 48090	102

Unclassified
Security Classification

DOCUMENT CONTROL DATA - R & D

(Security classification of title, body of abstract and indexing annotation must be entered when the overall report is classified)

1. ORIGINATING ACTIVITY *(Corporate author)*

University of Vermont
Burlington, Vermont

2a. REPORT SECURITY CLASSIFICATION

Unclassified

2b. GROUP

3. REPORT TITLE

The Fracture Energy of Composite Materials

4. DESCRIPTIVE NOTES *(Type of report and inclusive dates)*

Final Report September 1, 1967 - August 31, 1968

5. AUTHOR(S) *(First name, middle initial, last name)*

John O. Outwater
Michael C. Murphy

6. REPORT DATE	7a. TOTAL NO. OF PAGES	7b. NO. OF REFS
September 30, 1968	28	

8a. CONTRACT OR GRANT NO.	9a. ORIGINATOR'S REPORT NUMBER(S)
DAAA 21-67-C-0041	
b. PROJECT NO.	
c.	9b. OTHER REPORT NO(S) *(Any other numbers that may be assigned this report)*
d.	

10. DISTRIBUTION STATEMENT

Distribution of this document is unlimited

11. SUPPLEMENTARY NOTES	12. SPONSORING MILITARY ACTIVITY
	Picatinny Arsenal Dover, New Jersey

13. ABSTRACT

A study of the sources of the fracture energy and hence the brittleness of laminates shows that one of the parameters governing the usefulness of a filament as a reinforcement for a matrix is the debonding energy in shear, G_{II}, between the filament and the matrix. A novel method of measuring this value is described. Using this technique, values of G_{II} are determined for freshly drawn Pyrex rods with many different surface treatments embedded in anhydride cured epoxy resin. The effects of environment on G_{II} are shown and it is noted that all debonding energies tend to be substantially the same value after long exposure. The rate of decrease of G_{II} is essentially the same for all finishes and is linear down to a certain value when the rate of decrease is sharply reduced. The rate of decrease of G_{II} depends both on the humidity and the temperature.

14. KEY WORDS	LINK A		LINK B		LINK C	
	ROLE	WT	ROLE	WT	ROLE	WT
Fracture Mechanics						
Fracture Energy						
Fiber Stability						
Epoxy Resin						
Glass						
Surface Treatment						
Outwater, J. O.						
Vermont, University of						